# COMPARED COUPLED AND UNCOUPLED LAGRANGIAN PARTICLE TRACKING TO ASSESS THE WIND INDUCED BIAS OF ATMOSPHERIC PRECIPITATION GAUGES

ENRICO CHINCHELLA[1,2], ARIANNA CAUTERUCCIO[1,2], LUCA G. LANZA[1,2]
[1]*University of Genova, Dep. of Civil, Chemical and Environmental Engineering (DICCA), Genoa, Italy*
[2] *WMO Measurement Lead Centre "B. Castelli" on Precipitation Intensity, Italy*

** e-mail: enrico.chinchella@unige.it*

***Keywords:*** *Atmospheric precipitation, Wind-induced bias, URANS, LES, Particle tracking, Drag coefficient.*

Atmospheric precipitation is a key component of the hydrological cycle and has a direct impact on numerous aspects of society, it is therefore evident that its precise and meticulous measure is a requirement. Numerous types of precipitation gauges, using different measurement principles, are employed. They can be classified in two major categories: Catching type Gauges (CG) and Non-Catching type Gauges (NCG). Instruments in the first class collect precipitation inside a reservoir, quantifying its volume using mechanical principles, while the others use indirect methods able to sense individual hydrometeors without the need of any container.

Precipitation measurements are affected by various types of biases [1], depending on the gauge design and measuring principle. The action of wind is a typical environmental factor that is recognized as being responsible of significant measurement biases for both CGs and NCGs. First documented by Jevons [2], the wind-induced bias is common to all precipitation gauges and is produced by the complex aerodynamic interactions arising between wind, the instrument body, and the incoming hydrometeors. The bluff body behaviour of the gauge, producing strong velocity gradients and turbulence near its sensing area, affects incoming hydrometeors that may be diverted away or inside the gauge sensing area, resulting in a biased measure of the precipitation characteristics.

Quantification of the wind-induced bias may be achieved using different approaches: field intercomparisons, Wind Tunnel (WT) tests and numerical simulation. The latter has been largely employed in recent years, thanks to its lower cost and the capability of simulating a wide variety of environmental conditions. Although with different approaches, numerical simulation has been extensively used in the literature to quantify the wind-induced bias in case of the radially symmetric geometry of CGs. Recently, the same approach was applied to NCGs, that present a complex, non-radially symmetric shape requiring the introduction of wind direction as an additional variable. Additionally, they measure not only the cumulated volume of precipitation but also the size and fall velocity of each individual hydrometeor.

In this work, using the CFD and particle tracking capabilities of OpenFOAM, three different approaches are compared to assess the wind-induced bias of the Thies Laser Precipitation Monitor (LPM), a widely used NCG that employs a laser beam to detect incoming hydrometeors. The diameter is determined by measuring the magnitude of the beam power reduction, while fall velocity is obtained from the duration of the beam power reduction.

The aerodynamic response of this instrument for various combinations of wind speed (from 2 to 20 m/s) and direction (from 0° to 180°) is published in the work of Chinchella et al. [3]. Velocity fields over high resolution meshes (over 4M cells) were obtained running URANS simulation with a k-ω SST turbulence model and a local time stepping approach. Since a steady-state solution was sought, the local time stepping numerical scheme was chosen to significantly reduce the computational burden, without the need of resorting to a RANS approach. The k-ω SST model exploits the best performance of both the k-ε and k-ω models and has become an almost industry standard.

To better understand the role of turbulence, LES using the WALE turbulence model were run for selected wind speeds (5 and 10 m/s) and directions (0° and 90°) adopting meshes with much higher resolution (about 20M and 25M cells, respectively). To improve convergence, LES were initialized by running precursor URANS simulations over the finer meshes, and to evaluate mesh refinements, by computing the ratio between the turbulence integral length scale and cell size, shown to be above 10 for the entire domain, except very close to the gauge body.

Velocity fields obtained from both approaches were then used as input for the particle tracking models considered. Here both uncoupled and one-way coupled LPT models were employed. The first is run using the time averaged velocity field (from the URANS simulations or LES) as a frozen air flow pattern, meaning that trajectories are computed only after the CFD simulation is over, hence the name. For the one-way coupled model, instead, CFD and LPT simulations are computed at the same time, but only trajectories are influenced by the changes in the velocity field, while the presence of the airborne particles does not affect the flow.

Since the volume fraction of hydrometeors in the air during a precipitation event is generally low even for high precipitation rates [4], particle-to-particle interactions are very limited, at least close to the ground where gauges are located, and are therefore neglected in this work. Due to the typical time scale of a hydrometeor crossing the

computational domain, varying between about 0.1 and 1 seconds, the assumption of a steady state condition for the wind field is also in reasonable accordance with typical field conditions.

The primary factor that controls the trajectory of hydrometeors in a wind field is their drag coefficient ($C_D$). Estimation of the $C_D$ is not straightforward, and several attempts were carried out in the literature to identify suitable relationships with the particle dimension and/or the terminal velocity. Folland [5] proposed different relationships between the particles Reynolds number ($Re_p$) and $C_D$ for various $Re_p$ ranges. Khvorostyanov and Curry [6], proposed similar formulations for $C_D$ as a function of $Re_p$, obtained from experimental studies and analytical models, for drops, spheres and snow crystals, introducing a correction to account for turbulence. Following [7], the best-fit curve (see Figure 1a) of the raw data provided by [6] (grey line) was implemented in this work to calculate the drag coefficient for $Re_p > 320$, while the equations proposed by [5] were adopted for $Re_p \leq 320$.

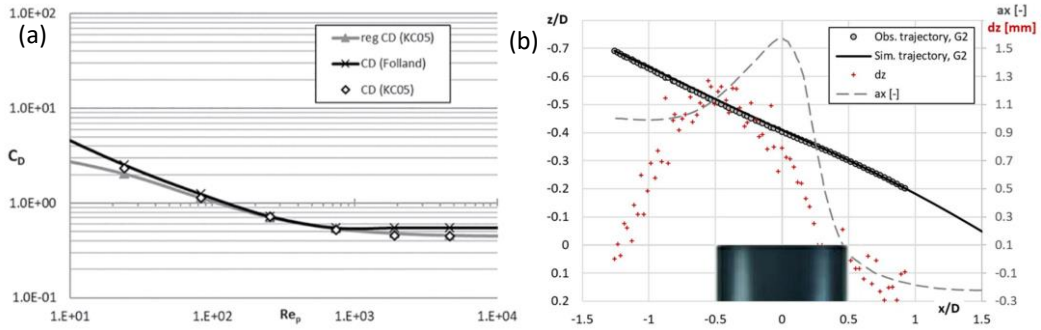


**Figure 1: (a) Comparison between the formulation by [5] (black line), the $C_D$ raw data provided in [6] (diamonds), and the best-fit curve (grey line) proposed in [7]. (b) WT validation of the simulated (solid line) drop trajectory with the observed one (circles) above the collector of a CG; the difference dz between the observed and simulated trajectories (red crosses) is reported together with the numerical longitudinal acceleration (ax) of the drop (dashed line)**

The uncoupled LPT model with the implemented $C_D$ formulation was validated in a previous work [7] by comparing simulated and measured water drop trajectories above the collector of two different CGs in WT experiments (Figure 1b). Drops of diameter between 0.7 and 1.2 mm were released in the WT using a precision volumetric pump and a calibrated nozzle, to generate single drops directly inside the flow upstream of the gauge. The trajectories of the released drops were captured using a high-speed camera. To highlight the deviation of drop trajectories when approaching the collector of the gauge, wind speeds between 9 and 13 m $s^{-1}$ were investigated in the WT. The validation based on the normalized differences, dz, between the simulation and the observed trajectory was satisfactory (see Table 2 in [7]) since the mean of the maximum value is about unity, with a low standard deviation (the coefficient of variation is about 0.4). Also, the mean and median values of dz are very similar, showing a symmetrical spread of these differences around the perfect agreement, which suggests quite a random nature of the error. Finally, the Root Mean Squared Difference is very low, always below $10^{-3}$, indicating an overall good agreement for all pairs of simulated and observed trajectories.

For all three LPT models considered (URANS-uncoupled, LES-uncoupled and LES one-way coupled), hydrometers were inserted in the domain along a variably spaced grid, considering 11 diameters between 0.25 mm and 8 mm. The grid is 0.25 m wide and 0.45 m long. It is positioned in the computational domain so that, for a constant wind field, the particle in its centre would fall perfectly in the middle of the instrument laser beam. Grid spacing varies between 10 mm and 0.625 mm and was determined running precursor simulations of the URANS-uncoupled model using a larger but coarser regularly spaced grid. Furthermore, for the uncoupled simulations, coincident with the instrument sensing area an internal surface was positioned within the mesh to represent the laser beam. For each particle, both its trajectory and impacting point on such virtual surface were saved for post-processing. For the one-way coupled simulation instead, no internal surface was inserted to avoid disrupting the flow, post-processing was therefore conducted only on the computed trajectories. Simulations were sopped only after all particles impacted the instrument, exited the domain or had fallen significantly below the instrument sensing area.

For each simulation, the Catch Ratio (CR), defined as the ratio between the number of hydrometers that successfully reached the instrument sensing area and the number of hydrometeors that would have reached se same area if no disturbance was present, is computed. This provides a quantitative evaluation of the instrument performance for a specific combination of drop size, wind speed and direction. Figure 2a shows the results for the uncoupled model applied to the URANS airflow simulation, while Figure 2b is obtained with the same LPT model on the LES results meanwhile Figure 2c shows the results of the one-way coupled model obtained evolving in time the LES alongside the LPT model. Results for the URANS-uncoupled model were fitted using a second-order inverse polynomial function and are presented in Figure 2 (dashed lines) for comparison.

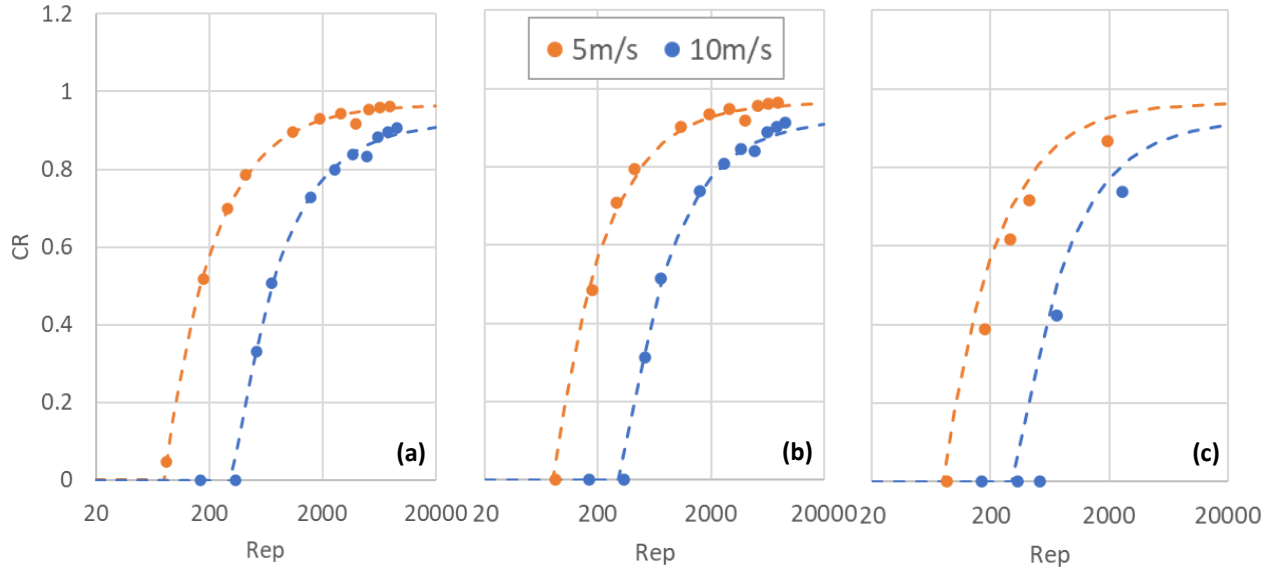


**Figure 2: Numerical catch ratios (symbols) for the LPM as a function of the particle Reynolds number at α = 0° using the (a) uncoupled URANS, (b) uncoupled LES, (c) coupled LES models. Dashed lines represent the best fitting curve for the results of the URANS-uncoupled approach**

Results are shown in terms of the Particle Reynolds Number ($Re_p$) and show that Cr increases with increasing $Re_p$ for all wind speeds with values that tend to unity for lower wind speeds and larger (and faster falling) drops. Smaller drops instead (that are the most common during precipitation) have Cr values that in some cases fall to zero, meaning that in those conditions the instrument is unable to detect any such small drop. The first two models (2a and 2b) are almost in perfect accordance, meaning that the increased computational burden of the LES does not provide any significant improvement over the URANS simulation using an uncoupled LPT model. Results of the one-way coupled model shows lower Cr values, meaning that the small-scale eddies have a non negligeable effect on the incoming hydrometeors. However, since this effect depends on the instantaneous flow velocity in the recirculation zone, which is intrinsically turbulent, the opposite effect may also be observed at another instant. This could be highlighted by running the simulation multiple times, while changing the instant when particles are released in the domain. Nevertheless, the high computational burden of such simulation limits the feasibility of the latter approach.

**Acknowledgements**

Simulations were run in the framework of the Italian CINECA Iscra projects named “CATCHLES – Scale resolving CFD simulation and particle tracking for non-catching type precipitation gauges” and “LESRAIN – LES-based particle tracking for non-catching rain gauges”.

**References**

[1] WMO – World Meteorological Organization, (2021): Guide to Instruments and Methods of Observation. WMO-N. 8, ISBN 978-92-63-10008-5.

[2] Jevons, W. S. (1861). LIV. On the deficiency of rain in an elevated rain-gauge, as caused by wind. The London, Edinburgh, and Dublin Philosophical Magazine and Journal of Science, 22(149), 421-433.

[3] Chinchella, E., Cauteruccio, A., Stagnaro, M., & Lanza, L. G. (2021). Investigation of the wind-induced airflow pattern near the Thies LPM precipitation gauge. Sensors, 21(14), 4880.

[4] Uijlenhoet, R., & Torres, D. S. (2006). Measurement and parameterization of rainfall microstructure. Journal of hydrology, 328(1-2), 1-7.

[5] Folland, C. K. (1988). Numerical models of the raingauge exposure problem, field experiments and an improved collector design. Quarterly Journal of the Royal Meteorological Society, 114, 1485–1516.

[6] Khvorostyanov, V. I., & Curry, J. A. (2005). Fall velocities of hydrometeors in the atmosphere: Refinements to a continuous analytical power law. Journal of the Atmospheric Sciences, 62, 4343–4357.

[7] Cauteruccio, A., Brambilla, E., Stagnaro, M., Lanza, L. G., & Rocchi, D. (2021). Wind Tunnel Validation of a Particle Tracking Model to Evaluate the Wind-Induced Bias of Precipitation Measurements. Water Resources Research, 57(7), e2020WR028766.